Aerosol Science and Technology
Publication details, including instructions for authors and subscription information:
http://www.tandfonline.com/loi/uast20

Design and Evaluation of a Plate-to-Plate Thermophoretic Precipitator

Chuen-Jinn Tsai [a] & Hsin-Chung Lu [a]
[a] Institute of Environmental Engineering, National Chiao Tung University , Hsin Chu, Taiwan
Published online: 26 May 2010.

To cite this article: Chuen-Jinn Tsai & Hsin-Chung Lu (1995) Design and Evaluation of a Plate-to-Plate Thermophoretic Precipitator, Aerosol Science and Technology, 22:2, 172-180, DOI: 10.1080/02786829408959738

To link to this article: http://dx.doi.org/10.1080/02786829408959738

Design and Evaluation of a Plate-to-Plate Thermophoretic Precipitator

Chuen-Jinn Tsai* and Hsin-Chung Lu
Institute of Environmental Engineering, National Chiao Tung University, Hsin Chu, Taiwan

A plate-to-plate thermophoretic precipitator with high particle collection efficiency has been designed and tested. The precipitator consists of two flat plates separated by a 0.38-mm thermal insulating shim. The top plate is heated by a constant high-temperature water flow while the bottom plate is cooled by a constant low-temperature water flow. Through this forced convective heat transfer arrangement, a high and uniform temperature gradient is achieved between the two plates, where submicron aerosol particles can be collected efficiently and uniformly in the direction of the air flow. The precipitator was tested in the laboratory using NaCl and sodium fluorescein monodisperse test particles. When the temperature gradient ranges from 502° to 879°C/cm and the Knudsen number ranges from 0.27 to 3.5, the experimental data show that the present precipitator collects submicron particles efficiently. Among previous theories, the thermophoretic velocity equation proposed by Talbot et al. (1980) is found to fit very well with the present experimental data.

INTRODUCTION

When an aerosol particle is suspended in a gas with a temperature gradient, the particle is subjected to a thermophoretic force and will move in the direction of decreasing temperature gradient. The thermophoretic phenomenon has been studied extensively both theoretically and experimentally (for example, Brock, 1962; Derjaguin and Yalamov, 1965, 1966; Derjaguin et al., 1966, 1976; Kousaka et al., 1976; Talbot et al. 1980; Nazaroff and Cass, 1987; Stratmann and Fissan, 1989; Bakanov, 1991; Montassier et al., 1991; Loyalka, 1992). In addition to air sampling applications, thermophoretic effect has also been used to suppress particle deposition to surfaces (Stratmann et al., 1988).

Swift and Lippmann (1989) has reviewed the previous design of thermophoretic precipitators for air sampling purposes. Green and Watson (1935) was the first to constructed a thermal precipitator of the heated wire design for measuring dust concentration. The flow rate is limited to 6–7 cm^3/min and the collection efficiency is low. Later, many modifications to the hot wire thermal precipitator were made mainly to increase the uniformity of the particle deposit. To increase particle collection efficiency further, Kethley et al. (1952) and Wright (1953) designed thermophoretic precipitators in which the temperature gradient is maintained by two circular plates. The aerosol is drawn through a tube in the center of the upper plate and flows radially in the gap between the plates. These precipitators are claimed to collect viable airborne particles efficiently but experimental data are very limited.

In the aspect of the thermophoretic theory, Brock (1962) was the first to do a

* To whom correspondence should be addressed.

0278-6826/95/$9.50
SSDI 0278-6826(94)00027-Y

Aerosol Science and Technology 22:172–180 (1995)

Published by Elsevier Science Inc.

complete hydrodynamic analysis of the problem. Later, Talbot et al. (1980) reviewed the previous theoretical work and found that Brock's equation (Brock, 1962) approaches Waldmann's free molecular limit for the thermophoretic force F_{th} (Waldmann, 1959, 1961), while other equations such as those proposed by Derjaguin and Yalamov (1965, 1966), and Derjaguin et al. (1976) do not. According to Derjaguin and Yalamov (1965, 1966), the thermophoretic velocity U_{th} is

$$U_{th} = \frac{3\nu \nabla T}{T_0}\left(\frac{k_g/k_p + C_t(\lambda/R)}{1 + 2(k_g/k_p) + 2C_t(\lambda/R)}\right). \tag{1}$$

Derjaguin et al. (1976) made a correction to the above equation with the factor 3 revised to 2.2.

Talbot et al. (1980) made a correction to Brock's fluid drag equation and proposed an interpolating formula for the thermophoretic velocity U_{th} as

$$U_{th} = \frac{2\nu C_s \nabla T C}{T_0(1 + 3C_m(\lambda/R))} \times \left(\frac{k_g/k_p + C_t(\lambda/R)}{1 + 2(k_g/k_p) + 2C_t(\lambda/R)}\right). \tag{2}$$

In the limit of very large Knudsen number, λ/R, Eq. 2 states that the dimensionless thermophoretic velocity, $U_{th}T_0/(\nu \nabla T)$ is a constant. Talbot et al. (1980) found that measurement in the particle-free layer over a heated flat plate, particle trajectory calculation according to Eq. 2 gave the best agreement with the experimental data. In Eqs. 1 and 2, R is the radius of the particle; λ is the mean free path of air molecules; $\nu = \mu/\rho$ is the air kinematic viscosity, with μ the air dynamic viscosity and ρ the air density; T_0 is the mean air temperature in the center of the particle; ∇T is the temperature gradient in the air; k_g and k_p are the thermal conductivities of the air and particle respectively; C is the slip correction factor; C_m is the momentum exchange coefficient; C_s is the thermal slip coefficient; and C_t is the temperature jump coefficient. For complete accommodation, the reasonable values of C_m, C_s, and C_t are 1.14, 1.17, and 2.18, respectively (Talbot et al., 1980; Montassier et al., 1991; Loyalka, 1992).

In the experimental study of thermophoretic particle deposition in laminar tube flow, Montassier et al. (1991) also found that Eq. 2 gives a good agreement between the experimental data and theoretical results. However, in the experiment of Montassier et al. (1991), the particle collection efficiency is very low, generally less than 10%. This may involves too much uncertainty in the measurement. In a recent study of thermophoretic force on a single particle by Loyalka (1992), the numerical solution of the linearized Boltzmann equation was obtained and compared with previous work. After reviewing many previous experimental results and theoretical work in the small Knudsen number regime, Bakanov (1991) concluded that differences among various theories still exist, and previous experimental results are not accurate enough to resolve these differences.

In this study, a plate to plate thermal precipitator of high particle collection efficiency has been designed and tested. The advantage of using two flat plates, the top of which is heated while the bottom is cooled by force convection, is that a high and uniform temperature gradient can be set up and hence particles can be collected efficiently on the colder bottom plate. Furthermore, since the relationship between the particle collection efficiency and thermophoretic precipitation velocity is simple for a laminar flow in a rectangular duct, it is easily to calculate the thermophoretic velocity from the measured particle collection efficiency data. In this study, the precipitator is tested for particle collection efficiency in the laboratory with two particle materials, namely NaCl and sodium fluorescein, under two high temperature gradients conditions. The experimental data converted in dimensionless form, $U_{th}T_0/(\nu \nabla T)$, can be used to check which of the previous thermophoretic theories is the most accurate one.

THE PLATE-TO-PLATE THERMAL PRECIPITATOR

A plate-to-plate thermal precipitator has been made and its detail drawing is shown in Figure 1. The thermal precipitation region is confined within a small gap between two flat plates, the top of which is heated by hot water circulating from a constant temperature bath while the bottom plate is cooled by water at ambient temperature. The precipitation area is 3.0 cm (W, width) $\times$ 7.1 cm (L, length), and the gap between the plates is kept at 0.38 mm (H, height) by a thermal insulating shim. The design air flow rate is kept constant at 0.4 L/min and the mean air velocity u_{av} is calculated to be 58.48 cm/s.

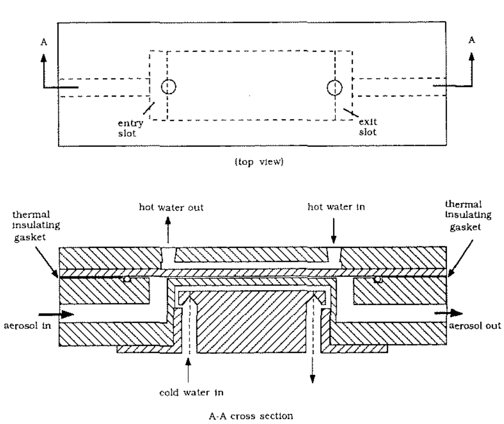

FIGURE 1. A schematic diagram of the present plate-to-plate thermophoretic precipitator.

The flow Reynolds number Re, defined as $\mathrm{Re} = \rho D_h u_{av}/\mu$ (D_h: hydrodynamic diameter), is 29.10 at ambient conditions. According to Schlichting (1979), the hydrodynamic entry length is $0.04\,\mathrm{Re}\,D_h = 0.087$ cm, which is very short compared with the channel length. Therefore the air flow can be considered to be laminar and fully developed in the precipitation region.

The temperature profile in the precipitation region is also fully developed since the Prandtl number is 0.7 for air flow and the temperature profile develops faster than the velocity profile. The theoretical temperature distribution and temperature gradient vertical to the flow direction can be calculated as discussed below.

According to the energy equation, one can obtain the following governing equation for the temperature distribution in the duct (refer to Figure 2 for the coordinate system) as

$$\rho c_p u \frac{\partial T}{\partial x} = k_g \frac{\partial^2 T}{\partial y^2}. \tag{3}$$

This equation can be solved for the temperature gradient dT/dy under constant heat flux conditions as

$$\frac{dT}{dy} = \frac{3\rho c_p u_{av}}{2k_g}\left(y - \frac{4y^3}{3H^2}\right)\frac{dT_m}{dx} + \frac{T_u - T_b}{H}. \tag{4}$$

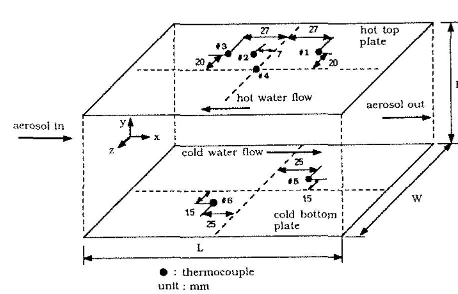

FIGURE 2. Coordinate system and the location of thermocouples.

In Eqs. 3 and 4, T_m is the mixing cup temperature, T_u and T_b are the top and bottom plate temperature, respectively, u_{av} is the average air velocity, c_p is the specific heat capacity of air at constant pressure. The mixing cup temperature T_m is defined as $T_m = \int_{-H/2}^{H/2} uTW\,dy / (u_{av} HW)$ where u and T are the air velocity and temperature at y. In this study, the temperature gradient is measured by six 0.2-mm diameter J-type thermocouples embedded in the top and bottom plates. Two sets of measured temperature data at air flow rates ranging from 0 to 7.43 L/min are shown in Table 1. For the positions where the thermocouples are installed, one can refer to Figure 2. It can be seen from the table that temperature distribution is very uniform along the direction of the precipitation region. For example, at the top portion of Table 1, it shows that the axial temperature variation dT_m/dx, only ranges from 0.17° to 0.20°C/cm in the top plate or from 0.06° to 0.08°C/cm in the bottom plate. The influence of air flow rate through the precipitator on the plate temperature is shown to be quite small, presumably because that the thermal conductivity of air is quite low compared with that of water. At the current design air flow rate of 0.4 L/min, the pressure drop through the precipitator, which is measured as 6 mm H_2O, can be considered to be very small.

Since the axial temperature variation is small, the first term of the right hand side of Eq. 4 is negligible compared with the second term. For example, referring to the data in the top portion of Table 1, at the air flow rate of 0.4 L/min and the average air temperature of 300 K, the maximum value of the first term of Eq. 4

TABLE 1. Experimental Temperature Data in the Thermophoretic Precipitator °C

Location Air Flow Rate (L/min)	Top Plate Point #1	Top Plate Point #2	Top Plate Point #3	Top Plate Point #4	Bottom Plate Point #5	Bottom Plate Point #6
0	39.2	38.8	38.1	38.3	22.3	22.0
0.4	39.1	38.8	38.1	38.4	22.3	22.0
1.49	39.2	38.8	38.2	38.4	22.2	21.9
2.97	39.2	38.7	38.2	38.4	22.2	21.8
4.46	39.1	38.8	38.2	38.3	22.2	21.9
5.94	39.2	38.8	38.1	38.2	22.2	21.8
7.43	39.1	38.7	38.1	38.2	22.2	21.8

Hot water tank temperature = 40.3°C, flow rate = 3.5 L/min
Old water inlet temperature = 20.8°C, flow rate = 0.77 L/min

Location Air Flow Rate (L/min)	Top Plate Point #1	Top Plate Point #2	Top Plate Point #3	Top Plate Point #4	Bottom Plate Point #5	Bottom Plate Point #6
0	29.8	29.4	29.2	29.4	21.5	21.3
0.4	29.8	29.5	29.2	29.4	21.5	21.4
1.49	29.8	29.5	29.2	29.4	21.5	21.3
2.97	29.6	29.3	29.0	29.3	21.3	21.1
4.46	29.8	29.4	29.2	29.3	21.4	21.3
5.94	29.8	29.5	29.1	29.3	21.4	21.2
7.43	29.8	29.6	29.2	29.2	21.4	21.3

Hot water tank temperature = 30.3°C, flow rate = 3.5 L/min
Cold water inlet temperature = 20.8°C, flow rate = 0.77 L/min

is about 5.0°C/cm, which is very small compared with the second term of 410°C/cm. Therefore, in this precipitator, the temperature gradient dT/dy can be considered to be uniform in both axial and vertical directions, and its value can be calculated directly from the measured top and bottom plate temperature data as

$$\frac{dT}{dy} = \frac{T_u - T_b}{H}. \qquad (5)$$

Therefore, a very high and uniform temperature gradient can be setup easily in this thermophoretic precipitator as long as the gap is kept small. It is expected that the particle collection efficiency will be high when the temperature gradient is raised to a high value. To find the particle collection efficiency η, the critical particle trajectory (x^*, y^*) for a particle to just deposit on the rear edge of the bottom plate must be found. Since the air flow becomes fully developed very quickly, one can assume a parabolic air velocity profile in the axial direction, and the particle equations of motion in the x and y directions can be written as

$$\frac{dy}{dt} = -U_{\text{th}},$$

$$\frac{dx}{dt} = \frac{3}{2}u_{\text{av}}\left(1 - \frac{4y^2}{H^2}\right). \qquad (6)$$

Integrating above equations and setting $x^* = L$, one can find the critical particle trajectory from the following equation as

$$y_* - \frac{4y_*^3}{3H^2} = \frac{2U_{\text{th}}}{3u_{\text{av}}}(L - x_*) - \frac{H}{3}. \qquad (7)$$

Setting $x^* = 0$ in the above equation, the critical point at the duct entry, y^*,, can be found from the following equation:

$$y_* - \frac{4y_*^3}{3H^2} = \frac{2U_{\text{th}}L}{3u_{\text{av}}} - \frac{H}{3} \qquad (8)$$

Then, the particle collection efficiency η can be calculated as

$$\eta = \frac{\int_{-H/2}^{y^*} \frac{3}{2}u_{\text{av}}\left(1 - \frac{4y^2}{H^2}\right)dy}{u_{\text{av}}H},$$

$$= \frac{3}{2H}\left(y_* + \frac{H}{2} - \frac{4y_*^3}{3H^2} - \frac{H}{6}\right),$$

$$= \frac{3}{2H}\left(\frac{2U_{\text{th}}L}{3u_{\text{av}}} - \frac{H}{3} + \frac{H}{2} - \frac{H}{6}\right),$$

$$= \frac{U_{\text{th}}L}{u_{\text{av}}H}. \qquad (9)$$

It is seen that particle collection efficiency η turns out to be the same as in the case of an uniform air velocity profile assumption. Using Eq. 9, the thermophoretic velocity U_{th} can therefore be calculated easily once the particle collection efficiency η is measured.

Besides high particle collection efficiency, there are additional advantages of using this thermophoretic precipitator. First, since the air flow is laminar in the precipitator, the precipitation flux of particles is uniform along the axial direction. Furthermore, since most of particles have thermal conductivity much higher than that of air, one can see from Eq. 2 that the precipitation velocity and hence the precipitation flux for submicron particles is nearly independent of particle materials. But this statement is not true for supermicron particles with high thermal conductivity.

EXPERIMENTAL METHOD AND RESULTS

The experimental setup used to measure the particle collection efficiency is shown in Figure 3. Polydisperse NaCl or sodium fluorescein aerosol is generated using a constant output aerosol atomizer (TSI model 3076). The aerosol is dried in a

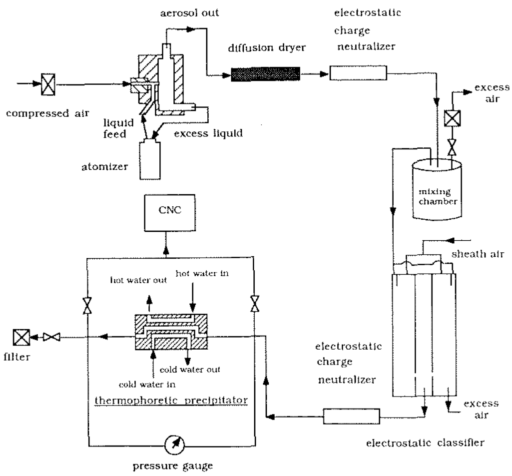

FIGURE 3. Schematic diagram of the experimental system.

diffusion dryer neutralized in an electrostatic charge neutralizer (TSI model 3077), and passed through an electrostatic classifier (TSI model 3071A) to generate monodisperse aerosol particles. The monodisperse aerosol is further neutralized by an electrostatic charge neutralizer before being introduced into the thermal precipitator. At a preset temperature gradient, the inlet and outlet aerosol concentrations are measured by a condensation nucleus counter (TSI model 3760). The particle collection efficiency is calculated from these concentration data. For the time being, the air flow rate through the precipitator is maintained at 0.4 L/min at ambient conditions.

In the experiment, particle loss due to Brownian diffusion is found to be important. When determining the particle collection efficiency due to thermophoretic effect, such particle loss has to be accounted for. Theoretical particle loss due to Brownian diffusion and gravitational settling in the thermal precipitation region can be seen in Table 2 for NaCl particles at the temperature gradient of 502.63°C/cm. The maximum theoretical particle loss, 6.5%, is due to Brownian diffusion, which occurs when the particle diameter is 0.04 μm. As can be seen in Table 2, the loss due to gravitational settling is negligible. In addition to the loss in the thermal precipitation region, it is found that loss of particles also occurs at other locations within the precipitator. The loss is particularly important at the entry and exit slots where flow may recirculate and the residence time of aerosol particles are much longer than that in the thermal precipitation region. The amount of this particle loss can't be predicted by theory and has to be determined experimentally.

The amount of total particle loss, η_L, was first determined experimentally by setting both the top and bottom plates at the same temperature. This temperature

TABLE 2. Particle Loss and Particle Collection Efficiency in the Thermophoretic Precipitator, NaCl Particles, Temperature Gradient = 502.63°C/cm

Dp (μm)	Diffusion Loss (%) (Theory)	Settling Loss (%) (Theory)	Total Loss η_L (%) (Experiment)	Total Measured Efficiency η_T (%)	Thermophoretic Efficiency η (%)
0.04	6.5	0.0	27.8	63.5	49.4
0.06	3.8	0.0	20.8	59.4	48.7
0.08	2.7	0.0	19.0	57.3	47.3
0.1	2.1	0.1	18.7	55.1	44.8
0.2	1.0	0.2	15.0	52.0	43.5
0.3	0.7	0.3	14.2	50.2	41.3
0.4	0.5	0.5	13.2	47.7	39.7
0.5	0.4	0.9	11.3	47.8	41.1

is the average between the top and bottom plate temperatures when the particle collection efficiency due to the thermophoretic effect, η, is to be determined at a certain temperature gradient. Total particle loss η_L was found to be much greater than the theoretical particle loss in the thermal precipitation region alone. It decreases from 27.8% to 11.3% when the particle diameter is increased from 0.04 to 0.5 μm.

After determining the total particle collection efficiency η_T which includes total particle loss, the thermophoretic precipitation efficiency, η, is then calculated as $1-(1-\eta_T)/(1-\eta_L)$.

The experimental collection efficiency due to thermophoretic effect is shown in Figure 4a for sodium fluorescein particles, and Figure 4b for NaCl particles at different thermal gradients. Temperature gradients are 526.3° and 878.96°C/cm for sodium fluorescein particles, 502.63° and 836.84°C/cm for NaCl particles, respectively. Experimental uncertainty which is represented as an error bar is also indicated in Figure 4. The tested particle diameter ranges from 0.04 to 0.5 μm and the thermal conductivities are 0.016 and 0.00103 cal/(cm·s·K) for NaCl (Reist, 1993) and sodium fluorescein (Montasier et al., 1991) respectively. It is seen that the particle collection efficiency increases as the thermal gradient is increased or when the particle size is decreased. Also in this precipitator, the collection efficiency for submicron particles is considered to be very high. For example, at the temperature gradient of 878.96°C/cm, the collection efficiency is above 75% for sodium fluorescein particles smaller than 0.2 μm in diameter. It is expected that higher collection efficiency than the present data can be obtained if the temperature gradient can be maintained above 890°C/cm.

When plotted using the coordinate of the dimensionless thermophoretic velocity, $U_{th}T_0/(\nu \nabla T)$, versus the Knudsen number, λ/R, Figure 5 shows the present experimental data agree very well with the theoretical predictions by Talbot et al. (1980) for both two particle materials at different temperature gradients. The data clearly show that $U_{th}T_0/(\nu \nabla T)$ approaches Waldmann's free molecular limit asymptotically as λ/R goes to infinity. Also shown for comparison is the theoretical prediction by Derjaguin and Yalamov (1965, 1966), which is represented by Eq. 1. The present experiment indicates that the theory by Derjaguin and Yalamov (1965, 1966) overestimates the thermophoretic velocity substantially in the range of the Knudsen number tested. Although not shown in Figure 5, the corrected for-

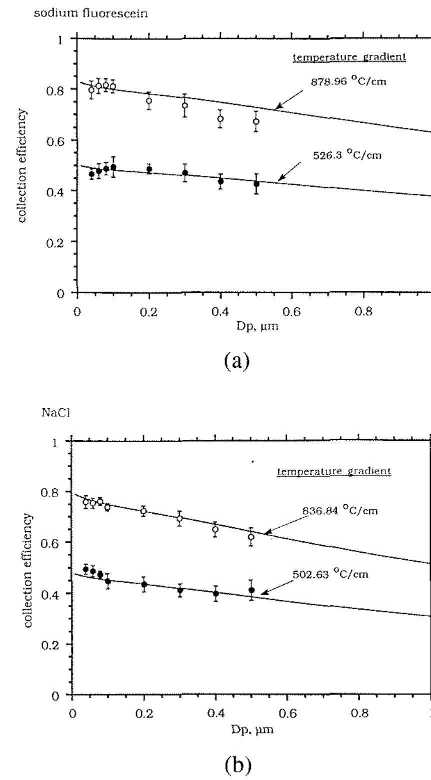

FIGURE 4. Particle collection efficiency in the precipitator at two different temperature gradients. (a) sodium fluorescein particles (b) NaCl particles.

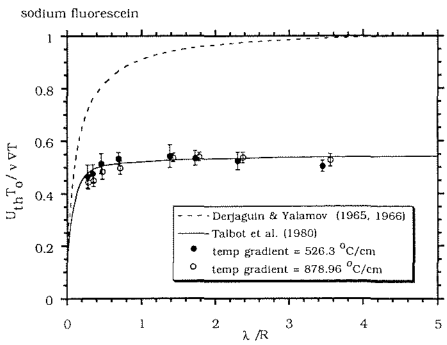

(a)

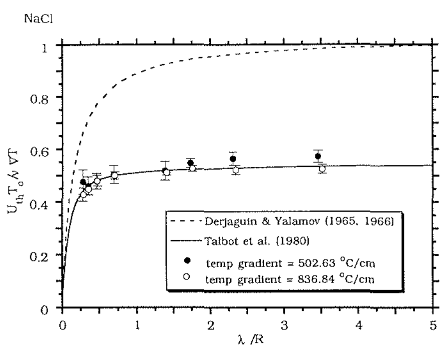

(b)

FIGURE 5. Comparison of experimental dimensionless thermophoretic velocities $U_{th}T_0/(\nu\nabla T)$ with theoretical prediction. (a) sodium fluorescein particles (b) NaCl particles.

mula by Derjaguin et al. (1976) also overestimates the thermophoretic velocity very much.

CONCLUSION

An efficient plate-to-plate thermophoretic precipitator has been designed and tested. Forced convective heat transfer through the top and bottom plates provides a high and uniform temperature gradient between plates, where submicron aerosol particles can be collected efficiently and uniformly in the direction of the air flow. The precipitator was tested in the laboratory using NaCl and sodium fluorescein monodisperse test particles at high thermal gradients. The present experimental data shows that the thermophoretic velocity formula proposed by Talbot et al. (1980) is accurate.

Since the particle collection efficiency is predictable using simple equations, the present precipitator can be used as an effective submicron aerosol sampling device. To increase sampling efficiency and flow rate further, the precipitation area or the temperature gradient can be increased from their present values. For example, it is easy to increase the present precipitation area of 21 cm^2 to a value dictated by the desirable collection efficiency and flow rate.

Using this plate to plate thermophoretic precipitator, more experimental data for low thermal conductivity materials and small Knudsen number flow can be obtained to further test various previous thermophoretic theories.

This research was supported by a contract number NSC-80-0410-E-009-22 with the National Science Council, Taiwan, Republic of China.

REFERENCES

Bakanov, S. P. (1991). *Aerosol Sci. Technol.* 15:77–92.

Brock, J. R. (1962). *J. Colloid Sci.* 17:768–780.

Derjaguin, B. V., and Yaramov, Yu. (1965). *J. Colloid Sci.* 20:555–570.

Derjaguin, B. V., and Yalamov, Yu. (1966). *J. Colloid Sci.* 21:256–258.

Derjaguin, B. V., and Storozhilova, A. I. and Rabinovich, Ya. I. (1966). *J. Colloid Interface Sci.* 21:35–58.

Derjaguin, B. V., Rabinovich, Ya. I., Storozhilova, A. I. and Scherbina, G. I. (1976). *J. Colloid Interface Sci.* 57:451–461.

Green, H. L., and Watson, H. H. (1935). *Med. Res. Council Spec. Rept.* No. 199, His Majesty's Stationary Office, London.

Kethley, T. W., Gordon, M. R., and Orr, C. (1952). *Science* 116:368–369.

Kousaka, Y., Okuyama, K., Nishio, S., and Yoshida, T. (1976). *J. Chem. Eng.* 9:147–150.

Loyalka, S. K. (1992). *J. Aerosol. Sci.* 23:291–300.

Montassier, N., Boulaud, D., and Renoux, A. (1991). *J. Aerosol Sci.* 5:677–687.

Nazaroff, W. W., and Cass, G. R. (1987). *J. Aerosol Sci.* 18:445–455.

Reist, P. C. *Aerosol Science and Technology*, 2nd ed., McGraw-Hill, New York, 1993.

Schlichting, H. *Boundary-Layer Theory*, 7th ed., McGraw-Hill, New York, 1979.

Stratmann, F., and Fissan, H. (1989). *J. Aerosol Sci.* 20:899–902.

Stratmann, F., Fissan, H., and Papperger, A. (1988). *Aerosol Sci. Technol.* 9:115–121.

Swift, D. L., and Lippmann, M. (1989). In Air Sampling Instruments for Evaluation of Atmospheric Contaminants, 7th ed. American Conference of Governmental Industrial Hygienists Inc., pp. 387–403.

Talbot, L., Cheng, R. K., Schefer, R. W., and Willis, D. R. (1980), *J. Fluid Mech.* 101:737–758.

Waldmann, L. (1959). *Z. Naturf.* 14:589–599.

Waldmann, L. (1961). In *Rarefied Gas Dynamics* (ed. L. Talbot), Academic, New York, p. 323.

Wright, B. M. (1953). *Science* 118:195.

Received February 8, 1994; revised May 11, 1994